# Spin state and orbital moments across the metal–insulator-transition of REBaCo2O5.5 investigated by XMCD

**M. Lafkioti, Eberhard Goering, S. Gold, G. Schütz, S. N. Barilo, S. V. Shiryaev, G. L. Bychkov, P. Lemmens, V. Hinkov, Joachim Deisenhofer, Alois Loidl**

**Angaben zur Veröffentlichung / Publication details:**

Lafkioti, M., Eberhard Goering, S. Gold, G. Schütz, S. N. Barilo, S. V. Shiryaev, G. L. Bychkov, et al. 2008. "Spin state and orbital moments across the metal–insulator-transition of REBaCo2O5.5 investigated by XMCD." New Journal of Physics 10 (12): 123030. https://doi.org/10.1088/1367-2630/10/12/123030.

# Spin state and orbital moments across the metal–insulator-transition of $REBaCo_2O_{5.5}$ investigated by XMCD

To cite this article: M Lafkioti *et al* 2008 *New J. Phys.* **10** 123030

New Journal of Physics
The open-access journal for physics

# Spin state and orbital moments across the metal–insulator-transition of $REBaCo_2O_{5.5}$ investigated by XMCD

**M Lafkioti[1], E Goering[1,6], S Gold[1], G Schütz[1], S N Barilo[3], S V Shiryaev[3], G L Bychkov[3], P Lemmens[4], V Hinkov[5], J Deisenhofer[2] and A Loidl[2]**

[1] Max Planck Institute for Metal Research, D-70569 Stuttgart, Germany
[2] Experimentalphysik V, Center of Electronic Correlations and Magnetism, Institute for Physics, Augsburg University, D-86159 Augsburg, Germany
[3] Institute of Solid State and Semiconductors, BAS, BY-220072 Minsk, Belarus
[4] Institute of Condensed Matter Physics, TU Braunschweig, D-38106 Braunschweig, Germany
[5] Max Planck Institute for Solid State Research, D-70569 Stuttgart, Germany
E-mail: goering@mf.mpg.de

*New Journal of Physics* **10** (2008) 123030 (9pp)
Received 23 July 2008
Published 18 December 2008
Online at http://www.njp.org/
doi:10.1088/1367-2630/10/12/123030

**Abstract.** $DyBaCo_2O_{5.5}$ has shown a complex phase diagram, which is based on the interplay of different energy scales, related to magnetism, orbital ordering and for example Co spin-state transitions. For a detailed understanding of these fascinating materials it is therefore necessary to identify the order of the different energy scales. Small changes in the corresponding energy relations strongly influence the electronic structure and ground state properties, like low and high spin configurations, which have been controversially discussed in order to interpret the metal-to-insulator (MIT) transition in $REBaCo_2O_{5.5}$ (RE = rare earths). To clarify unambiguously the microscopic nature of the spin-state evolution associated with this MIT, we performed detailed temperature and angular dependent x-ray magnetic circular dichroism measurements in $DyBaCo_2O_{5.5}$ single crystals above and below the MIT and at the onset of the ferromagnetic phase. Anisotropic contributions of spin and orbital moments have been observed with an extremely high signal-to-noise ratio. We can identify a higher-spin- to lower-spin-state change across the MIT, which is in contrast

[6] Author to whom any correspondence should be addressed.

to previous macroscopic experimental findings. Only the Co ions in octahedral environment are found to be in a reduced spin configuration in the high-temperature metallic state.

**Contents**



## 1. Introduction

The fascinating physical properties of transition metal oxides originating from the complexity of the coupling of the spin, charge, orbital and lattice degrees of freedom, have attracted considerable interest in the last few years. The resulting phenomenology ranges from metal-to-insulator transitions (MITs) [1] and the colossal magnetoresistance (CMR) effects, e.g. in manganites [2] and cobaltates [3] to high-temperature superconductivity in cuprates [4, 5]. Cobalt-based oxides have revealed their own microcosms within this manifold of phenomena [3], [6]–[14] and came to the fore because of the occurrence of temperature-dependent spin-state changes of the Co ions, which are based on the delicate relation between the crystal field and Hund's rule coupling energy.

In particular, the recently discovered layered $REBaCo_2O_{5.5}$ compounds show a series of magnetic transitions, which evidence the competing ferromagnetic (FM) and antiferromagnetic (AFM) interactions at lower temperatures. In addition, enormous uniaxial magnetocrystalline anisotropy (MCA) has been observed, which suggests the presence of an unusual high unquenched orbital moment, experimentally not yet observed. Nevertheless, the main attention is concentrated on the observation of a MIT above room temperature, accompanied by a change in the susceptibility, indicating correlated-electron phenomena [1]. The special oxygen stoichiometry of these systems allows a stable oxygen-deficient structure with $Co^{3+}$ ions in octahedral and pyramidal coordination to occur (see figure 1). In principle, three spin configurations are possible for each $Co^{3+}$ site, depending on the competition of crystal-field splitting and Hund's rule coupling: high spin (HS: $S = 2$, $t_{2g}^4 e_g^2$), intermediate spin (IS: $S = 1$, $t_{2g}^5 e_g^1$) and low spin (LS: $S = 0$, $t_{2g}^6$). Therefore, the Co ions in different coordinations can have various spin states with different temperature dependence, accounting for the MIT.

The interpretation of the susceptibility change at the MIT is rather controversial. Maignan *et al* [9, 10] suggested that at $T < T_{MI}$ the octahedral $Co^{3+}$-ions are in a LS and the pyramidal ones in an IS state, whereas at $T > T_{MI}$ the $Co^{3+}$-ions at both Co sites change to HS. Taskin *et al* on the other hand [3, 13] claim that, as a result of thermal expansion and higher entropy of the HS state, the octahedra are in the HS state above the MIT, whereas the pyramids remain in

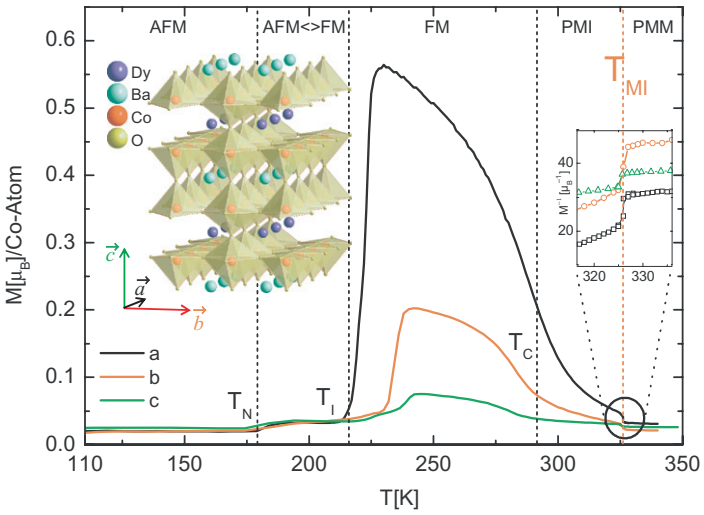


**Figure 1.** Crystal structure of $DyBaCo_2O_{5.5}$ (data from [21]) and SQUID magnetization measurements at $H = 2\,\mathrm{T}$ as a function of temperature along the three crystallographic axes $a$ (black), $b$ (red) and $c$ (green). Inset: inverse magnetization at the MI-transition at 326 K.

the IS state [6]. These scenarios are based on the assumption of paramagnetic (PM) behaviour around the MIT and attempt to model the experimentally observed change in the slope of the inverse magnetic susceptibility $\chi^{-1}$ [3, 6], [8]–[10], [13]. Apart from the lack of microscopic information to support or discard either of these scenarios, the implied assumption that the $Co^{3+}$ ions at the octahedral site may possibly be in a LS ground state is in contradiction to recent LSDA + U calculations [14].

Therefore, we performed x-ray magnetic circular dichroism (XMCD) measurements on a detwinned single crystal of $DyBaCo_2O_{5.5}$ to directly determine the behaviour of spin- and orbital-moment contributions at different temperatures and, thereby, provide microscopic magnetic information about the spin state transition and the MIT. Our results will show that the octahedral $Co^{3+}$ ions perform a change to a lower spin state above the MIT, in contradiction to previous experimental suggestions. The results shown here provide a deep understanding of the magnetic properties and the MIT, consistent with the theoretical model by H Wu [14], where hole delocalization effects of the Co ions are considered. Our findings resolve present discrepancies between theoretical and experimental results.

## 2. Experimental

All XMCD spectra were measured in total electron yield (TEY) mode at the BESSY II bending magnet beamline PM3 with our own dedicated XMCD system in an applied magnetic field of 2 T. All sum-rule-related values were corrected for the finite circular polarization of $0.93 \pm 0.02$. The monochromator energy resolution was set to $E/\Delta E \approx 6000$ to obtain the optimal compromise between intensity and energy resolution. With our XMCD system, we have achieved an extraordinarily high XMCD signal-to-noise ratio of up to 17 000 with respect to the total absorption signal. This was only possible by flipping the magnetic field at every data point, to successfully reduce synchrotron based drift phenomena. In addition, all

results were performed for both light helicities to reduce even smallest possible contributions from non-XMCD-related difference signal. This enables very sensitive XMCD measurements even for diluted paramagnets far above the ordering temperature [15, 16]. Further details of the experimental setup and the data handling procedure have been described elsewhere [16, 17].

The measured single crystal of $DyBaCo_2O_{5.5}$ was grown from flux [18] and annealed in flowing oxygen [19]. The crystals were cut in a rectangular shape and polished.

As grown $DyBaCo_2O_{5.5}$ single crystals are twinned due to the similarity of the in-plane lattice constants [19], i.e. they consist of equal proportions of nearly orthogonally oriented domains. To allow the investigation of the anisotropy, we detwinned the sample by subjecting it to uniaxial stress at elevated temperature [20] and characterized it using magnetic susceptibility measurements and polarized light microscopy. The residual degree of twinning has been determined to be 25% (see figure 1 and section 3.1). For the XMCD measurements the detwinned $DyBaCo_2O_{5.5}$ single crystal was cleaved *in situ* under ultra high vaccum (UHV) conditions.

## 3. Results

### *3.1. SQUID*

To characterize the crystal we performed field-cooled magnetization measurements recorded with a commercial quantum design SQUID magnetometer, with an applied magnetic field of 2 T along the three crystallographic axes $a$, $b$ and $c$ (see figure 1). From the shown curves, we determined the residual degree of twinning to be ∼25%. The PM dysprosium contribution has been subtracted beforehand [3]. The different magnetic transitions with temperature agree well with literature [9, 13]. The AFM ground state is followed by an intermediate phase (AFM <> FM) above the Neél-temperature $T_N = 179$ K, where AFM and FM order compete up to the onset of a FM phase at $T_I = 230$ K. Above $T_C \approx 292$ K, the system enters a PM insulating (PMI) phase [9, 22]. Finally, the sharp step in the magnetization at $T_{MI} = 326$ K indicates the transition into the high-temperature PM metallic (PMM) state [3, 9, 10, 13, 23].

In the following, we will focus on the MIT, but we point out that the magnetic structure of the low temperature phases below $T_C$ is still under strong debate [12], as is the spin state across the MIT [3], [24]–[28]. At the MIT, the net magnetic moment is reduced by about 40%, with the main drop of $13 \times 10^{-3}\ \mu_B$/Co-atom occurring along the $a$-axis. The step along the $c$-axis of $3.09 \times 10^{-3}\ \mu_B$/Co-atom is very small, and of the same order of magnitude as the $b$-axis step after correction of residual twinning effects. The extraordinary sharpness of the MIT with a transition width of about 1 K verifies the O-content of 5.5 in the crystal [13] and gives evidence for the high quality of the sample. According to literature, where the spin state interpretation is based on the slope of the inverse susceptibility, one would expect an increase of the magnetization at the MIT, due to a LS (IS) to HS change of the octahedral Co ions, whereas the pyramids remain in the IS (HS) state [3, 6], [8]–[10], [13]. In our case the discontinuity in the inverse magnetization curve (inset in figure 1 showing $M^{-1}$) forbids a simple PM state analysis and a corresponding slope based moment determination close to the MIT [9, 23]. To understand this step of the magnetization and its origin it is necessary to go further into the microscopic magnetic behaviour.

### *3.2. XMCD*

To achieve an element specific determination of the Co 3d spin and orbital moments across the MIT, we studied the projected Co sample magnetization at the Co $L_{2,3}$ edges using XMCD [29]–[31]. The XMCD signal is the difference between the two x-ray absorption spectra (XAS) measured with light helicity parallel and antiparallel to the sample magnetization, to obtain the projected spin and orbital moments of the Co-atoms using so called sum rules [32, 33]. Due to the fact that one cannot simply magnetically saturate the sample in a PM phase along all measured crystallographic directions, we only present XMCD related effective magnetic spin moments $2\langle s_z\rangle + 7\langle T_z\rangle$, where a fraction of this spin could be due to the magnetic dipole term [34]. As we are predominately investigating the PM phases of a $DyBaCo_2O_{5.5}$ crystal at about 40–50 K above the Curie temperature, complete sample saturation needs at least 100 T, which is not possible for low-noise XMCD measurements so far. However, for the determination of relative magnetic-moment changes in a PM phase, saturation is not necessary. Saturation can in principle be important in terms of the MIT, due to possible long range magnetic order, but the MIT appears at relatively high temperatures far in the PM phase, with related small magnetization and magnetic ordering parameters. Therefore, magnetic long range order is not responsible for the MIT, which is also supported by the field independent temperature position of the MIT [13].

To gain insight into these relative changes and the microscopic origin of the magnetization behaviour we recorded XMCD-spectra along the *a*- and *c*-axes in three different magnetic phases, namely in the FM 245 K (black curve), the PMI 315 K (red) and the PMM phase 345 K (blue) shown in figure 2. The changes in the XMCD signal with increasing temperature are clearly observable, along with the MIT and its dependence on the crystallographic direction. The relative decrease of the XMCD signal at the $L_3$-edge from the FM to the PMI phase and across the MIT is quantitatively consistent with the magnetization data shown in figure 1. The easy-axis behaviour along the *a*-axis is evident (compare figures 2(a) and (b)), as is the XMCD signal reduction by a factor of 2 (315 K $\rightarrow$ 345 K) across the MIT. As a result of the high signal-to-noise ratio we are able to resolve the XMCD substructure of the $L_3$ edge.

## 4. Discussion

Figure 3 shows the magnified XAS $L_3$-edge region and related peak-normalized XMCD spectra, in order to clarify the MIT-induced changes in the spectral shape. The *a*-axis-related XAS also exhibit a small shift of 0.12 eV in spectral weight to lower energy (arrows in figure 3(b)), according to a band gap reduction at the MIT. Spectroscopic results by Hu *et al* have already shown that $Co^{3+}$ in an octahedral (LS) coordination has a shoulder on the high-energy side, while pyramids (HS) with the same valence state exhibit a shoulder at the low-energy side (see XAS results of Hu *et al* and [7]). Compared to [7] pyramidal configurations at lower spin states should provide a shift to lower energies, based on the reduced exchange/CF-energy-ratio, whereas higher spin states at the octahedral site will provide a shift to higher energies, based on the increased exchange/CF-energy-ratio. According to this picture of crystal field and exchange energy related states, one would expect a conserved separation between the octahedral and the pyramidal states observed in x-ray absorption spectroscopy [36].

For the system investigated here, the density of states (DOS) calculations from Wu exhibit similar energy variations of the unoccupied DOS between the pyramids and the octahedra [37].

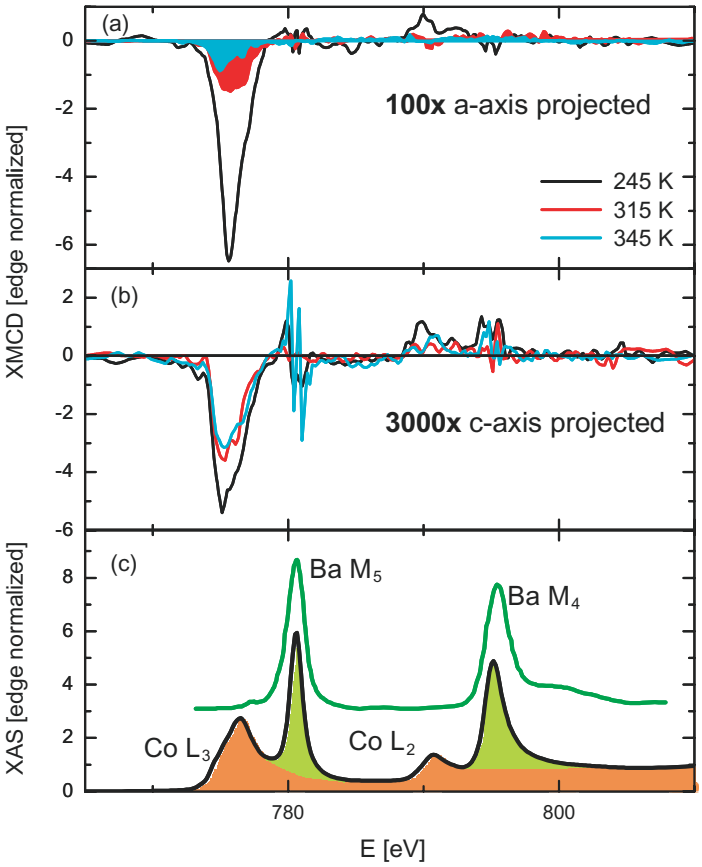


**Figure 2.** XMCD spectra along the *a*-axis (a) and *c*-axis (b) at 245 K in the FM phase (black), below 315 K (red) and above $T_{MI}$ 345 K (blue). (c) XAS along the *a*-axis. In addition, the Ba $M_{4,5}$ spectrum from [35] is reproduced and shifted for better visibility.

Therefore, the $L_3$-edge high-energy substructure is consistently identified to originate from the octahedral Co ions (yellow shaded in figure 3), and the low-energy part from the pyramidal ones (green shaded in figure 3) [7], with an overlapping region in between, related to both of them. The strong reduction of the octahedral part at the MIT (see also figure 3), in comparison with the low energy substructure (pyramids), gives further evidence for a reduced magnetization at the octahedra in the PMM state as proposed by Wu [14]. In particular, below $T_{MI}$ the low-energy part along the *a*-axis has about the same intensity as the high-energy part, but the relative intensity changes from about 2 : 2 (at 775 eV) to 2 : 1 (at 776.5 eV) across $T_{MI}$, enforcing the following results about the microscopic moments. This leads to an interpretation of the spin state transition located at the octahedral $Co^{3+}$-ions from a higher spin-state configuration (HS or IS) below $T_{MI} = 326$ K to a lower spin-state configuration (IS or LS, respectively) above the MI-transition.

We have applied conventional Co $L_{2,3}$ edge sum rules [32, 33] to investigate the temperature dependence of spin and orbital moments along the crystallographic *a*- and *c*-axes separately. For the standard Co $L_{2,3}$ XAS intensity approximation [38], we have estimated and removed the Ba $M_{4,5}$ XAS intensity as shown in figure 2(c), according to measurements of the

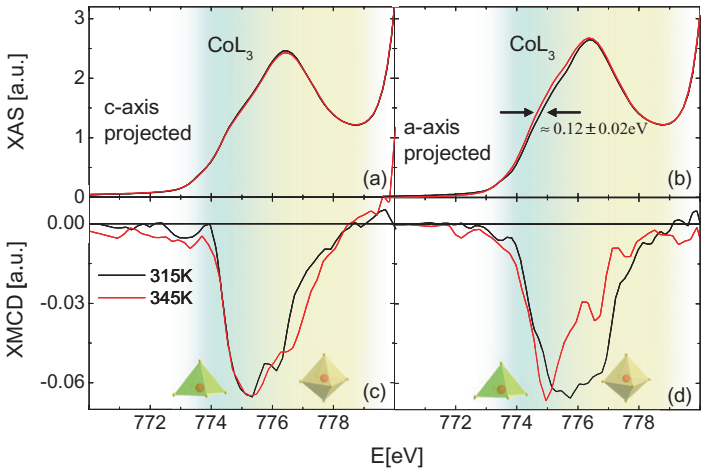


**Figure 3.** Enlarged XAS- and peak-normalized XMCD-spectra above (below) the MIT shown as a red (black) line at the Co $L_3$ edge along the *a*- (right) and *c*-axes (left). Two major things happen at the MIT: the nonmagnetic spectral weight, close to the transition threshold, shifts in energy (indicated by the arrows in (b), and a change of the XMCD spectral shape in (d). Pyramidal and octahedral spectral weight is indicated by the symbols and shading.

Ba $M_{4,5}$ edge on $BaF_2$ [35]. The Ba 4f shell is empty in both cases (our spectrum and the $BaF_2$) resulting in a nonmagnetic 4f configuration. The reproduced Ba $M_{4,5}$ spectrum is therefore representative and in good agreement with our Ba-contribution estimated here.

We found a small PM (PMI and PMM) *c*-axis-projected spin moment of $1.5 \pm 0.1 \times 10^{-3}\,\mu_B$/Co and an orbital moment of $0.6 \pm 0.1 \times 10^{-3}\,\mu_B$/Co, both remaining constant across the MIT. Along the easy *a*-axis, a higher spin moment of $73 \pm 1.8 \times 10^{-3}\,\mu_B$/Co and an orbital moment of $32 \pm 2.9 \times 10^{-3}\,\mu_B$/Co were observed in the FM phase at 245 K, which decrease, respectively, to $28 \pm 2.5 \times 10^{-3}\,\mu_B$/Co and $8.6 \pm 3.6 \times 10^{-3}\,\mu_B$/Co at 315 K in the PMI phase. The large absolute orbital-to-spin-moment ratios and their anisotropic expectation values, as observed here, are the microscopic origin of the very strong macroscopic MCA, which does not vanish in the PM phases [39]–[42]. Both $s_z$ and $l_z$ decrease by about 50% to $s_z = 13 \pm 1.2 \times 10^{-3}\,\mu_B$/Co and $l_z = 4.3 \pm 1.8 \times 10^{-3}\,\mu_B$/Co, respectively, across the MIT. This suggests that in the FM phase the octahedrally and pyramidally coordinated Co ions are both of HS or IS character and a LS state at the octahedral sites below the MIT can be excluded. Due to the fact that the spin–orbit ratio is not changing significantly across the MIT, the vanishing moment has to have the same spin–orbit ratio as the remaining one. This leads us to the conclusion that both sites have the same configuration in the FM and PMI phases.

In the following, we try to identify which configurations (HS, IS and LS) are present at the various temperatures. Just from the high-temperature effective magnetic moments of $4.3\,\mu_B$, determined by a Curie–Weiss fit of the inverse susceptibility above the MIT, one can consistently reproduce this value by a mixture of a HS–IS configuration providing $2.83\,\mu_B + 4.9\,\mu_B/2 = 3.87\,\mu_B$ and additional orbital magnetization, as shown above [6]. This indicates a transition from a low temperature HS–HS to a high-temperature HS–IS configuration. Nevertheless, this transition type should result in a change of the spin–orbital moment ratio, which is clearly not observable here. In addition, this spin state assignment also implies that the slope based

determination of the magnetic moment is valid for a highly anisotropic PM state. Following the arguments given in section 3.1, we do not believe that this is simply correct here, clearly questioning the correct relation of the determined absolute values (4.3 $\mu_B$) with the expected HS–IS (3.87 $\mu_B$) result.

Taking also into account that the large orbital moments, present in PMI and PMM phases, have been theoretically identified as an IS configuration with a hole in the $t_{2g}\, d_{xz}$ orbital [24], we can consistently identify the MIT as an IS–IS (PMI) to IS–LS (PMM) transition. This is also consistent with the spin–orbital moment ratio, which remains constant across the MIT.

The reduction of the magnetic moment occurs consistently in the SQUID and XMCD measurements, proving that the widely held assumption of a LS to HS transition at the octahedral sites with a concomitant creation of a HS-conduction band cannot be the reason for the MIT [3, 9, 13]. The observed large orbital moment below the MIT ($T < T_{MI} = 326$ K) can be explained by an IS state of $Co^{3+}$-ions at pyramidal and octahedral sites. While above the MIT, the octahedrally coordinated $Co^{3+}$-ions are in a LS state, the pyramidal sites remain in the IS state. This explains the reduction of the spin and orbital moments by 50% across the MIT. The origin of the metallic phase should now be found in the delocalization of the O-pd $\sigma$ holes, as results from the theoretical study of Wu *et al*, consistent with the reduced crystal field [14].

## 5. Summary

We have performed low-noise XMCD measurements of $DyBaCo_2O_{5.5}$ in the FM and the two PM insulating and metallic phases, i.e. below and above the MIT transition of this material. The XMCD signal has been determined with a noise level down to $50 \times 10^{-6}\, \mu_B$. Large orbital moments have been found, providing a microscopic understanding of the unusual strong anisotropic behaviour in this system. The high-energy spectral weight of the XMCD signal vanishes at the MIT, identifying an octahedral LS state in the high temperature PMM phase. Our XMCD results definitely exclude the spin state transition at the MIT of $DyBaCo_2O_{5.5}$ from being of low to higher spin character, which is in contradiction to the majority of interpretations published so far. We identify the spin state transition at the MIT in the $REBaCo_2O_{5.5}$ system as an IS to LS transition located at the octahedral Co ions. Our results eliminate inconsistencies between present experimental findings and theoretical LDA + U calculations [14].

## Acknowledgments

We authors thank B Ludescher for technical assistance. We would also like to acknowledge BESSY II and T Kachel for the support at the beamline and the Max Planck Society for financial support. We acknowledge partial support by the BMBF via contract number VDI/EKM 13N6917 and by the DFG via SFB 484.

## References

[1] Imada M, Fujimori A and Tokura Y 1998 *Rev. Mod. Phys.* **70** 1039–263
[2] Solovyev I V 2003 *Phys. Rev. Lett.* **91** 177201
[3] Taskin A A, Lavrov A N and Ando Y 2003 *Phys. Rev. Lett.* **90** 227201
[4] Chu C W, Gao L, Chen F, Huang Z J, Meng R L and Xue Y Y 1993 *Nature* **365** 323–5
[5] Ramirez A P 1999 *Nature* **399** 527–8

[6] Frontera C, Garcia-Munoz J L, Llobet A and Aranda M A G 2002 *Phys. Rev.* B **65** 180405
[7] Hu Z *et al* 2004 *Phys. Rev. Lett.* **92** 207402
[8] Khalyavin D D, Barilo S N, Shirayaev S V, Bychkov G L, Troyanchuk I O, Furrer A, Allenspach P, Szymczak H and Szymczak R 2003 *Phys. Rev.* B **67** 214421
[9] Maignan A, Martin C, Pelloquin D, Nguyen N and Raveau B 1999 *J. Solid State Chem.* **142** 247–60
[10] Maignan A, Caignaert V, Raveau B, Khomskii D I and Sawatzky G A 2004 *Phys. Rev. Lett.* **93** 026401
[11] Flavell W R 2005 *J. Electron Spectrosc. Relat. Phenom.* **144–147** 777–82
[12] Soda M, Yasui Y, Fujita T, Miyashita T, Sato M and Kakurai K 2003 *J. Phys. Soc. Japan* **72** 1729–34
[13] Taskin A A, Lavrov A N and Ando Y 2005 *Phys. Rev.* B **71** 134414
[14] Wu H 2003 *J. Phys.: Condens. Matter* **15** 503
[15] Tietze T, Gacic M, Schuetz G, Jakob G, Brueck S and Goering E 2008 *New J. Phys.* **10** 055009
[16] Gacic M, Jakob G, Herbort C, Adrian H, Tietze T, Brueck S and Goering E 2007 *Phys. Rev.* B **75** 205206
[17] Goering E, Gold S, Bayer A and Schütz G 2001 *J. Synchrotron Radiat.* **8** 434–6
[18] Chernenkov Y P, Plakhty V P, Gukasov A G, Barilo S N, Shiryaev S V, Bychkov G L, Hinkov V, Feodorov V I and Chekanov V A 2007 *Phys. Lett.* A **365** 166–70
[19] Streule S, Podlesnyak A, Mesot J, Medarde M, Conder K, Pomjakushina E, Mitberg E and Kozhevnikov V 2005 *J. Phys.: Condens. Matter* **17** 3317–24
[20] Hinkov V, Pailhes S, Bourges P, Sidis Y, Ivanov A, Kulakov A, Lin C T, Chen D P, Bernhard C and Keimer B 2004 *Nature* **430** 650–4
[21] Frontera C, Garcia-Munoz J L, Carrillo A E, Aranda M A G, Margiolaki I and Caneiro A 2006 *Phys. Rev.* B **74** 054406
[22] Roy S, Khan M, Guo Y Q, Craig J and Ali N 2002 *Phys. Rev.* B **65** 064437
[23] Frontera C, Garcia-Munoz J L, Llobet A, Aranda M A G, Rodriguez-Carvajal J, Respaud M, Broto J M, Raquet B, Rakoto H and Goiran M 2002 *J. Magn. Magn. Mater.* **242–245** 751–3
[24] Pardo V and Baldomir D 2006 *Phys. Rev.* B **73** 165117
[25] Khalyavin D D, Argyriou D N, Amann U, Yaremchenko A A and Kharton V V 2007 *Phys. Rev.* B **75** 134407
[26] Khalyavin D D 2005 *Phys. Rev.* B **72** 134408
[27] Fauth F, Suard E, Caignaert V and Mirebeau I 2002 *Phys. Rev.* B **66** 184421
[28] Plakhty V P, Chernenkov Y P, Barilo S N, Podlesnyak A, Pomjakushina E, Moskvin E V and Gavrilov S V 2005 *Phys. Rev.* B **71** 214407
[29] Stöhr J and Siegmann H C 2006 *Magnetism: From Fundamentals to Nanoscale Dynamics* (Berlin: Springer)
[30] Schütz G, Wagner W, Wilhelm W, Kienle P, Zeller R, Frahm R and Materlik G 1987 *Phys. Rev. Lett.* **58** 737–40
[31] Schütz G, Goering E and Stoll H *Synchrotron Radiation Techniques* ed H Kronmuller and S Parkin (Chichester: Wiley) p 1311
[32] Carra P, Thole B T, Altarelli M and Wang X 1993 *Phys. Rev. Lett.* **70** 694–7
[33] Thole B T, Carra P, Sette F and van der Laan G 1992 *Phys. Rev. Lett.* **68** 1943–6
[34] Stöhr J and König H 1995 *Phys. Rev. Lett.* **75** 3748–51
[35] Eberhardt W, Colbow K M, Gao Y, Rogers D and Tiedje T 1992 *Phys. Rev.* B **46** 12388–93
[36] Cox P A 1992 *Transition Metal Oxides* (Oxford: Clarendon)
[37] Wu H 2001 *Phys. Rev.* B **64** 092413
[38] Chen C T, Idzerda Y U, Lin H J, Smith N V, Meigs G, Chaban E, Ho G H, Pellegrin E and Sette F 1995 *Phys. Rev. Lett.* **75** 152–5
[39] Gold S, Goering E, König C, Rüdiger U, Güntherodt G and Schütz G 2005 *Phys. Rev.* B **71** 220404
[40] Goering E, Bayer A, Gold S, Schütz G, Rabe M, Rüdiger U and Güntherodt G 2002 *Phys. Rev. Lett.* **88** 207203
[41] van der Laan G 1998 *J. Phys.: Condens. Matter* **10** 3239–53
[42] Bruno P 1989 *Phys. Rev.* B **39** R865–8